ATTENUATION OF GAMMA RADIATION THROUGH TWO-LEGGED RECTANGULAR DUCTS AND SHELTER ENTRANCEWAYS — AN ANALYTICAL APPROACH

TN-383

20 January 1961

U. S. NAVAL CIVIL ENGINEERING LABORATORY

Port Hueneme, California

ATTENUATION OF GAMMA RADIATION THROUGH TWO-LEGGED RECTANGULAR DUCTS AND SHELTER ENTRANCEWAYS — AN ANALYTICAL APPROACH

Y-F011-05-329

Type C

by

J. C. LeDoux*, A. B. Chilton

OBJECT OF TASK

To improve existing knowledge on gamma and neutron shielding properties of shelters.

ABSTRACT

An analytical approach is developed to permit determination of gamma radiation attenuation as it passes through two-legged rectangular ducts and shelter entranceways. The approach used employs the albedo concept for wall scattering and includes correction terms necessary to account for the "corner lip effect." With appropriate simplifying assumptions, moderately simple engineering formulas are obtained. Actual use of the formulas requires better knowledge of differential angular albedo than is presently available; however, by assuming isotropic distribution of the albedo function, a very good comparison of experimental information with results calculated by this technique is obtained.

* Now stationed at the U. S. Naval School, Civil Engineer Corps Officers, Port Hueneme, California

CONTENTS

CONTENTS (Cont'd)

I. INTRODUCTION TO THE PROBLEM

The problem of designing a shield against nuclear radiation such as gamma rays and neutrons is essentially one of interposing sufficient mass of material between the source of radiation and the detector. Both gamma rays and neutrons exhibit an approximate exponential attenuation behavior in passing through matter, so that complete removal of all the radiation is impossible. The amount of radiation has to be reduced to a level consistent with the purpose of the shield. The design of such a shield would be relatively simple if either the source of radiation or the shield space could be completely surrounded by the proper thickness of shielding material. This is not possible since practical considerations require that some means of access to the source or shielded space must be made. Thus a reactor core must have control rods, conduits, etc. A personnel shelter must have utility and ventilation ducts and personnel entranceways.

The problem is to be able to design these access ducts so that the level of radiation outside the radiation source enclosure or inside a shelter is not significantly increased by the installation of these ducts and openings. It has frequently in the past been the practice merely to place one or two 90-degree bends in ducts without any very careful analysis, to provide necessary attenuation. With rather thick shielding walls and small ducts this practice has proved adequate. However, for a large duct, such as an entranceway into a shelter, this crude approach is inadequate. The design of such an entranceway will probably depend greatly on its nuclear radiation transmission properties, and since entranceways are an expensive component of a shelter, careful analysis is very worthwhile.

It is the purpose of this note to analyze the transmission of gamma rays through rectangular ducts from basic scattering principles, using largely the "albedo" concept. In so doing, there are two ends in view. The first is to lay down a set of tentative analytical techniques to be used by nuclear engineering designers concerned with this problem, pending further refinement of the art; the second is to provide some theory which experimental programs carried out by NCEL (and other organizations) can undertake to check.

It may also be possible to obtain some sound knowledge of how the radiation attenuation factors vary with the geometric scale of the physical layout. Such a knowledge may be useful in permitting analysis of large-scale entranceways through small-scale experiments. Therefore, comments on the scaling relationships will be provided where something meaningful can be said.

II. ANALYSIS OF THE BASIC PROBLEM

A. The Albedo Concept

The basic application of the albedo concept to this sort of problem is not new (see, for example, Ref. 1). For the sake of the reader not too familiar with its use in such a case, the following review is presented.

Consider an idealized basic situation in which an isotropic point source emits radiation, and a detector is situated such that it responds only to radiation scattered from a small plane area, A. By "small" area, we mean that its linear dimensions are much less than r_1, the distance from source to the area, and r_2, the distance from the area to the detector. (See Figure 1.)

A set of cartesian coordinate axes is established with the origin within A, and in such a way that the Z-axis is normal to the plane of the area A, and the point source is in the X-Z plane. In addition to the radial distance r_1, the position of the source is indicated by the angle from the normal θ_1. Obviously, there is no reason to expect the detector to be in the X-Z plane necessarily, and thus, in addition to the radial distance r_2, the two angles θ_2 and ϕ are required to establish its position.

If appropriate means are provided to eliminate any passage of radiation from source to detector except by scattering off A, and if there is no attenuation by media in the path from-source-to-area-to-detector, the detector reading is readily seen to be (Ref. 1, page 335):

$$D = \frac{D_o \; A \; \bar{a} \; \cos\theta_1}{r_1^{\,2} \; r_2^{\,2}} \tag{1}$$

where D_0 is a detector response in the direct beam, at one unit of distance from the source; and $\bar{a} \equiv \bar{a}(\theta_1, \theta_2, \phi)$ is the "differential directional albedo" (hereinafter referred to as the "differential albedo"),

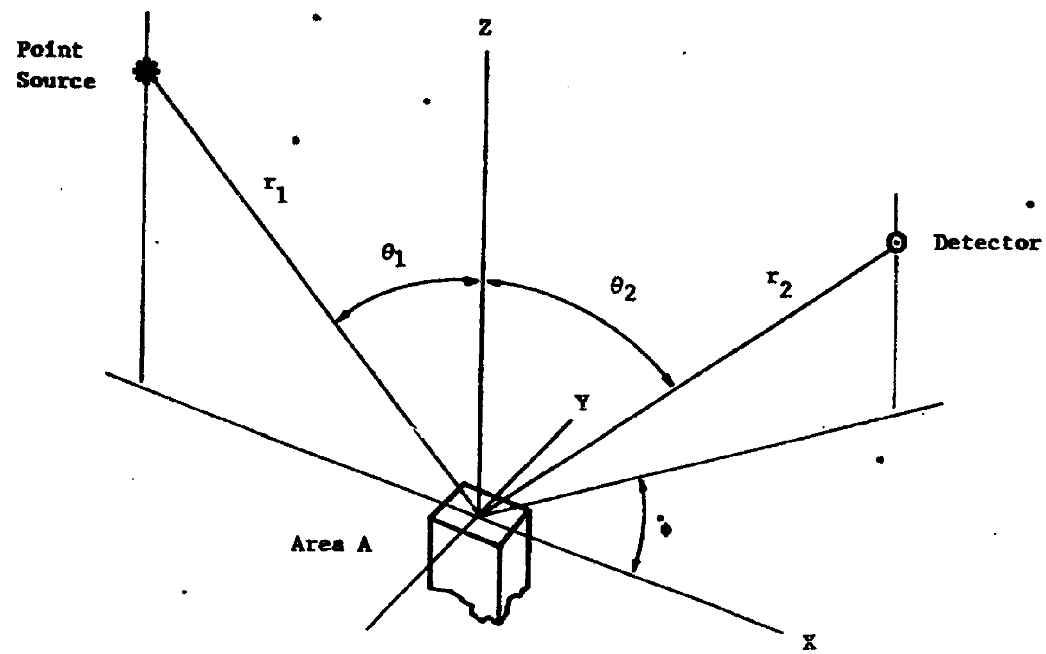

Figure 1. Scattering of gamma rays from surface.

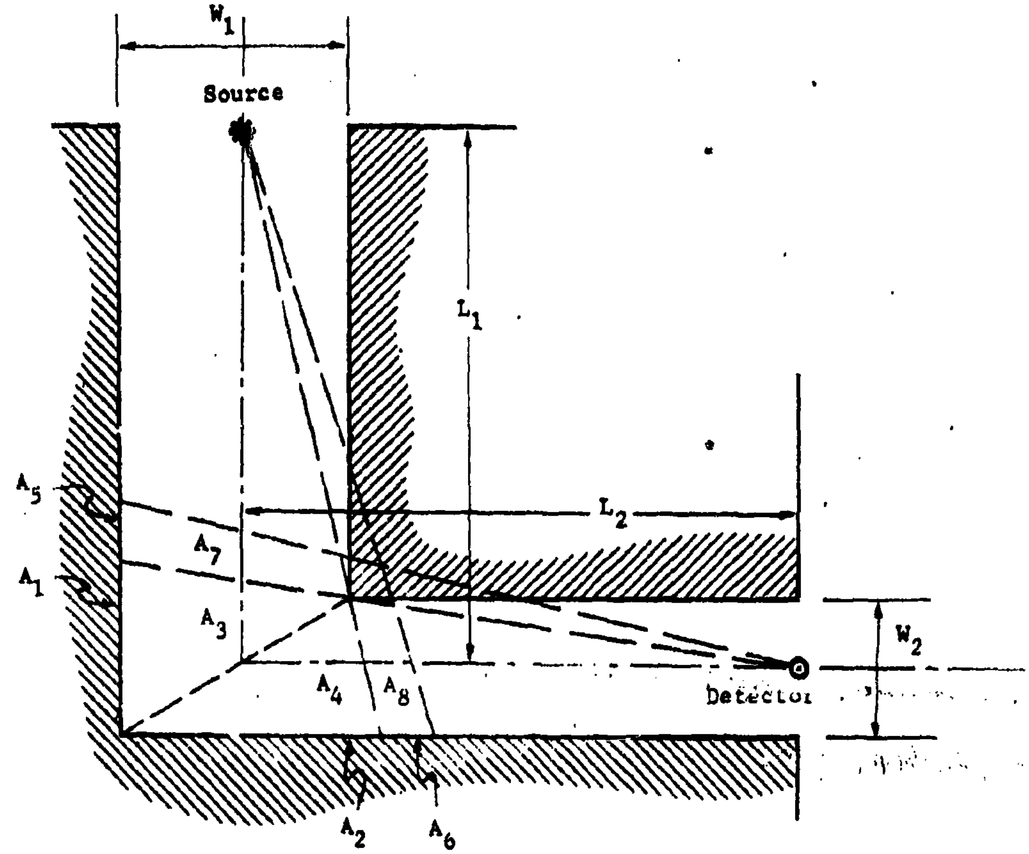

Figure 2. Duct geometry indicating prime and transmission scattering areas.

or reflection factor, for the radiation. In addition to the geometric angular factors, the differential albedo depends also on the energy of the incident radiations and the nature of the scattering material under the surface of A. It gives the proportion of radiation incident on A which is reflected off in the given direction, per steradian.

If D and D_o are numbers of particles (or photons), $\bar{a}$ must be a "number albedo"; if, on the other hand, the detector measures radiation energy flux, D and D_o represents energy and $\bar{a}$ is an "energy albedo"; finally, if D and D_o indicate "dose," $\bar{a}$ is a "dose albedo."

There is available at present considerably more information on "total albedo," the proportion of radiation scattered in toto, than on the "differential albedo," which is that scattered into specific directions. If information is only available on total albedo, one must make some assumptions as to the actual distribution with emergent angles θ_2 and ϕ. For example, if an isotropic assumption is made, Equation 1 becomes:

$$D = \frac{D_o \; A \; a_T}{2\pi \; r_1^2} \frac{\cos\theta_1}{r_2^2} \tag{2a}$$

where $a_T \equiv a_T(\theta_1)$ is the total albedo factor for the radiation energy and reflecting material considered, and

$$a_T(\theta_1) = \int_{\text{upper hemisphere}} \bar{a}(\theta_1, \theta_2, \phi) \; \sin\theta_2 \; d\theta_2 \; d\phi \tag{2b}$$

If a number of scattering areas of different orientation are involved, the detector dose becomes:

$$D = D_o \sum_i \frac{\bar{a}(\theta_{i1}, \theta_{i2}, \phi_i) \; A_i \; \cos\theta_{i1}}{r_{i1}^2 \; r_{i2}^2} \tag{2c}$$

B. Approach and Assumptions

The basic problem to be solved is depicted in Figure 2. This shows a two-legged duct, with legs intersecting perpendicularly, having a rectangular cross section. The height of the rectangle, H, is the dimension perpendicular to the plane of the paper in the figure; it is taken to be the same for both legs — a usual situation. The transmission of radiation through the duct will be calculated first with the assumption that only those areas which can be seen by both the source and the detector are important. The case is considered to be the "basic" case; its solution is the first approximation to the total solution; the scattering areas involved are called "prime" scattering areas and are shown as areas A_1 through A_4, inclusive, in Figure 2. Areas 1 and 2 are wall areas; areas 3 and 4 each include both roof and floor.

Although the discussion is made with gamma rays primarily in mind, the formulas derived are applicable to any type of radiation which reasonably conforms to the assumptions.

At this basic stage in the development of the theory, scattering off one surface only will be considered. Multiple scattering effects, to the degree they are significant, are discussed in Section V-C.

A certain degree of approximation will be necessary in order to provide some mathematical simplicity. Correction terms on the order of 10 percent or greater will be retained, those of the order of a few percent or less will be ignored.

Some simplifications are possible if certain dimensional symmetries or equalities are assumed or if simple expressions for the albedo factors are assumed. For the present analytical development these are not assumed, so that the expressions derived will be generally useful.

It is assumed that the leg lengths are appreciably greater than the widths and the height. More precisely, the length of the shorter leg should be at least three or four times the width of the wider leg (or height) for assured accuracy. Also, to minimize direct transmission of radiation from source to detector, both legs should not be less than a few feet in length.

It is assumed that the leg dimensions are much less than a mean free path of the radiation in air, so that interaction with the air may be considered negligible.

All the linear dimensions of the duct, such as width and height, are on the order of or greater than a mean free path of the radiation in the material of which the walls are composed. This requirement, for example, would indicate that the smallest duct through concrete to which the analysis is applicable would have a width and height of several inches.

The wall materials are uniform in composition and density, especially at the corner. If the wall is made of a liner of some material imbedded in another material, the liner has a thickness on the order of or greater than a mean free path of the radiation in the liner material.

The radiation source is located at the center of the duct entrance; the detector is located at the center of the duct exit. Under the assumptions given, a slight variation away from the center line of the duct for either source or detector should not cause too great a variation in results. Furthermore, a source distributed over the mouth of the duct entrance may be considered as concentrated in the assumed spot without severe inaccuracy, provided D_o is appropriately calculated for such a case.

Most of the above restrictive assumptions may be relaxed to some degree without introducing serious inaccuracies. However, the exact degree of approximation in so doing is not thoroughly studied and is largely left for the future.

C. Basic Calculation

The basic calculation will consider scattering from areas A_1 through A_4, inclusive. (Areas in the plane of the paper are doubled so as to account for both top and bottom surfaces.) These areas are readily obtained from geometrical considerations and are listed in Table I.

The values of $\cos\theta_1$, as required in Equation 1, are also readily obtained and are given in Table I. In making this computation for each area, the radiation is considered to strike, on the average, a point whose location is conveniently expressed mathematically and which roughly approximates the centroid of the area.

The values of r_1 and r_2 in Equation 1, as well as the symbol denoting the proper value of the albedo factor, for the areas in question are given in Table II.

From these quantities and the use of Equation 1, the doses resulting from the various areas are readily arrived at, and are listed in Table III.

Table I. Area and Angle Parameters in Analysis of Basic Problem and Lip Transmission Effect

Area Designation	Value of Area	Value of $\cos\theta_1$ (Eq. 1)
1	$\frac{W_2\ H}{1 - \beta_1}$	$\frac{W_1}{2\ L_1}$
2	$\frac{W_1\ H}{1 - \beta_2}$	1
3	$\frac{W_1\ W_2}{1 - \beta_1}$	$\frac{H}{2\ L_1}$
4	$\frac{W_1\ W_2}{1 - \beta_2}$	$\frac{H}{2\ L_1}$
5	$\frac{W_2\ H\ (1 + \beta_1)}{2\ \mu_a'\ L_2\ (1 - \beta_1)^2}$	$\frac{W_1}{2\ L_1\ (1 - \beta_2)}$
6	$\frac{W_1\ H\ (1 + \beta_2)}{2\ \mu_a\ L_1\ (1 - \beta_2)^2}$	1
7	$\frac{W_1\ W_2}{\mu_a'\ L_2\ (1 - \beta_1)^2}$	$\frac{H}{2\ L_1\ (1 - \beta_2)}$
8	$\frac{W_1\ W_2}{\mu_a\ L_1\ (1 - \beta_2)^2}$	$\frac{H}{2\ L_1}$

Note: $\beta_1 = \frac{W_1}{2\ L_2}$, $\beta_2 = \frac{W_2}{2\ L_1}$, $\beta_3 = \frac{H}{2\ L_2}$

Table II. Distance and Albedo Parameters in Analysis of Basic Problem and Lip Transmission Effect

Area Designation	Mean Distance		Albedo Factor
	From Source	From Detector	
1	L_1	$L_2\ (1 + \beta_1)$	a_1
2	$L_1\ (1 + \beta_2)$	L_2	a_2
3	L_1	L_2	a_3
4	L_1	L_2	$a_4\ (\cong a_3)$
5	$L_1\ (1 - \beta_2)$	$L_2\ (1 + \beta_1)$	a_5
6	$L_1\ (1 + \beta_2)$	$L_2\ (1 - \beta_1)$	a_6
7	$L_1\ (1 - \beta_2)$	L_2	a_7
8	L_1	$L_2\ (1 - \beta_1)$	a_8

Note: $\beta_1 = \frac{W_1}{2\ L_2}$, $\beta_2 = \frac{W_2}{2\ L_1}$, $\beta_3 = \frac{H}{2\ L_2}$

Table III. Dose Contributions From Areas Involved in Basic Analysis and Lip Transmission Effect

Area Designation	Dose Contribution
1	$\dfrac{D_o W_2 H a_1 W_1}{2 L_1^3 L_2^2 (1 + \beta_1)}$
2	$\dfrac{D_o W_1 H a_2}{L_1^2 L_2^2 (1 + \beta_2)}$
3	$\dfrac{D_o W_1 W_2 a_3 H}{2 L_1^3 L_2^2 (1 - \beta_1)}$
4	$\dfrac{D_o W_1 W_2 a_4 H}{2 L_1^3 L_2^2 (1 - \beta_1)}$
5	$\dfrac{D_o W_2 H W_1 a_5}{4 \mu_a' L_2^3 L_1^3 (1 - \beta_2)^3 (1 - \beta_1)}$
6	$\dfrac{D_o W_1 H a_6}{2 \mu_a L_1^3 L_2^2 (1 - \beta_1)^2 (1 - \beta_2)}$
7	$\dfrac{D_o W_1 W_2 H a_7}{2 \mu_a' L_2^3 L_1^3 (1 - \beta_2)^3 (1 - \beta_1)^2}$
8	$\dfrac{D_o W_1 W_2 H a_8}{2 \mu_a L_1^4 L_2^2 (1 - \beta_1)^2 (1 - \beta_2)^2}$

The total dose expected from the prime scattering areas is summed from the contributions of the four areas and is given as follows:

$$D_{basic} = \frac{D_o W_1 W_2 H}{2 L_1^3 L_2^2} \left\{ \frac{a_1}{1 + \beta_1} + \frac{a_2}{\beta_2 (1 + \beta_2)} + \frac{a_3}{1 - \beta_1} + \frac{a_4}{1 - \beta_2} \right\} \quad (3a)$$

or

$$D_{basic} = D_1 (4 \beta_1 \beta_2 \beta_3) (G_b) \quad (3b)$$

where

$$\left.\begin{aligned} D_1 &= \frac{D_o}{L_1^2} \\ \beta_1 &= \frac{W_1}{2 L_2} \\ \beta_2 &= \frac{W_2}{2 L_1} \\ \beta_3 &= \frac{H}{2 L_2} \\ G_b &= \frac{a_1}{1 + \beta_1} + \frac{a_2}{\beta_2 (1 + \beta_2)} + \frac{a_3}{1 - \beta_1} + \frac{a_4}{1 - \beta_2} \end{aligned}\right\} \quad (3c)$$

a_1, a_2, a_3, and a_4 are the differential dose albedos from prime areas 1, 2, 3, and 4, respectively.

It is to be noted that D_1 is the theoretical dose expected (without wall scattering effects) at the corner, that is, where the mid-lines of the two legs intersect. It is useful to separate out this particular factor, since certain effects can be approximated by appropriate modifications to this term. This will be seen later.

It is obvious from a glance at Equation 3b that the last two factors are nondimensional, and that for a given geometrical configuration, their product is independent of any scale selection. Under circumstances which allow this basic analysis to be an adequate approximation, the scaling-independence of this part of the expression permits ready adaptation of experimental solutions on a small model scale for solution of large-scale problems of this nature. (Possibly important correction factors may make this more difficult, however, as we shall see presently.)

III. CALCULATIONS OF CORRECTIONS FOR VARIOUS CORNER LIP EFFECTS

A. General

Certain important other effects are desirable to consider, for in some cases they are quite important compared to results of the basic computation, even under circumstances in which the assumptions listed in Section II.B are met. These effects are related to the existence of the so-called corner "lip," and their inclusion in the analysis constitutes a sort of "first-order" correction to the basic solution.

B. Corner Lip Transmission Effects

In the basic calculation it is assumed that the corner lip (the inner edge of the intersection of the two legs) is completely opaque to the radiation. This can never be precisely true, and in some cases radiation penetration of the lip can be quite significant.

If it is assumed that radiation absorption of a ray passing through the lip is exponential in character, one can show on an elementary basis that the amount of radiation passing through the lip is the same as if all the radiation within a certain cut-off point were transmitted and all beyond it were absorbed. Furthermore, the distance of travel within the lip material of that particular ray passing exactly through the cut-off point can be shown to be the reciprocal of the effective attenuation coefficient for the radiation passing through it (assuming the use of an "effective attenuation coefficient" for dose absorption is valid). Appendix I shows the proof of these statements.

The simplest assumption for an effective absorption coefficient is that which accounts for all energy-absorbing processes and assumes that all energy scattered but not absorbed is scattered through a negligibly small angle. The use of the "energy absorption coefficient" gives thus a reasonable value to use in this regard.

On this basis, then, the effect of corner-lip penetration can be readily approximated by an increase in the scattering area beyond the primary scattering areas. The areas on Figure 2 which are designated A_5 through A_8, inclusive, show the new scattering surfaces which contribute to detector response, through the albedo process. The calculation of the values of these areas and other variables required to determine their effect, according to Equation 1, is straightforward and is summarized in Tables I, II, and III, along with previously mentioned data for the basic area contributions.

It is convenient to break up this lip transmission effect contribution into two parts: one in which wall scattering occurs before lip transmission, and the other in which lip transmission occurs before wall scattering. We find then that

$$D_{tr} = D_{tr1} + D_{tr2}$$

where

$$D_{tr1} = \frac{D_o W_1 W_2 H}{2 L_1^3 L_2^2} \left\{ \frac{(1 - \beta_1) a_5 + 2 a_7}{2 \mu_a' L_2 (1 - \beta_1)^2 (1 - \beta_2)^3} \right\} \tag{4a}$$

$$= D_1 (4 \beta_1 \beta_2 \beta_3) G_{t1} \tag{4b}$$

$$G_{t1} = \frac{(1 - \beta_1) a_5 + 2 a_7}{2 \mu_a' L_2 (1 - \beta_1)^2 (1 - \beta_2)^3} \tag{4c}$$

and $$D_{tr2} = \frac{D_o W_1 W_2 H}{2 L_1^3 L_2^2} \left\{ \frac{(1 - \beta_2) a_6 + 2 \beta_2 a_8}{2 \mu_a L_1 \beta_2 (1 - \beta_1)^2 (1 - \beta_2)^2} \right\} \tag{5a}$$

$$= D_1 (4 \beta_1 \beta_2 \beta_3) G_{t2} \tag{5b}$$

$$G_{t2} = \frac{(1 - \beta_2) a_6 + 2 \beta_2 a_8}{2 \mu_a L_1 \beta_2 (1 - \beta_1)^2 (1 - \beta_2)^2} \tag{5c}$$

D_1 has been previously defined by the set of Equations 3c. μ_a is the energy absorption coefficient of the primary radiation, μ_a' is the coefficient of the radiation reflected from the surfaces. See Table IV for numerical data on these coefficients.

It is to be noted that in Equations 4b and 5b the two latter terms of each equation are nondimensional; however, the product of these two terms is not independent of the geometric scale selection but is inversely proportional to the scale size. We note that the attenuation coefficients are fixed and do not change value with a change in geometric scale. Since the scaling relationships for similar factors in the basic problem and this particular correction are not the same, the problem of scaling up from model experiments to larger-scale prototypes is seen to be impossible unless some way is found to separate experimental data into the basic part and the lip-effect terms, or unless the lip-effect terms can be shown to be negligible at all scales considered.

D_{tr1} and D_{tr2} can be added to give

$$D_{tr} = D_1 (4 \beta_1 \beta_2 \beta_3) G_t \tag{6a}$$

where $$G_t = G_{t1} + G_{t2} \tag{6b}$$

Table IV. Nuclear Quantities Used in Duct Attenuation Formulas

E_o (Mev)	μ_a' (cm^{-1})	μ_a (cm^{-1})	$\left(\frac{Z\ N}{\mu_a^2}\right) r_o^2$	Material
0.50	.0473	.0473	17.00	
1.25	.0473	.0434	20.10	Earth (100 pcf)
6.00	.0473	.0300	45.70	
0.50	.0695	.0695	11.55	
1.25	.0695	.0630	13.70	Concrete (145 pcf)
6.00	.0695	.0442	31.30	
0.50	.3140	.2240	3.38	
1.25	.2450	.1900	4.68	Iron (475 pcf)
6.00	.2260	.1742	5.47	
0.50	6.260	1.120	1.68	
1.25	2.545	0.375	1.51	Lead (705 pcf)
6.00	1.318	0.422	1.19	

Note #1. The absorption coefficients (μ) for earth and concrete are relatively constant in the ranges 0.2 - 0.6 Mev and 4 - 10 Mev, which cover the significant ranges of energy for single 90-degree scattered and initial bomb radiation spectra, respectively.

Note #2. The absorption coefficients are inversely proportional to the density of material with roughly the same average atomic number. For densities different than those listed use the ratio: $\mu\rho/\rho_o$, where ρ is the actual density and ρ_o the density listed in this table. The same thing is true of the term $\left(\frac{Z\ N}{\mu_a^2}\right) r_o^2$.

C. Corner Lip In-Scattering Effect

Not only may the corner lip transmit some of the radiation photons (or particles) completely, but it may also serve to scatter some of them one or more times in the passage. Such scattering will in part redirect radiation toward the detector. Thus the detector not only "sees" the prime and additional scattering areas on the outer walls by means of their radiation scatter, but also "sees" the corner lip as a "bright" source — almost a line source.

In analyzing the contribution of this effect we make certain simplifications. In similar spirit to that used in the preceding section we utilize an "effective attenuation coefficient" for radiation passing to and from each scattering center, thus again using what might be considered a "straight-ahead approximation." The previous approach is modified to the extent that we recognize a small but definite probability of scattering into the direction which will cause the radiation to hit the detector. Thus we have a single-scatter approximation for the most part, but the approach does not eliminate multiple scattering provided all the scattering processes but one are considered of a small angle nature. Scattering through two or more appreciable angles of large amount is considered of negligible proportion (an approximation which is admittedly not entirely valid for photons or particles of quite low energy).

The computation of the effect for gamma ray photons is based on the Klein-Nishina scattering formula (Ref. 2). Its use in this particular case is explained in detail in Appendix II. The results of the detailed analysis are as follows:

$$D_s = \frac{D_o\ W_1\ W_2\ H\ Z\ N\ K}{4\ L_1^3\ L_2^3\ \mu_a^2\ (1 - \beta_1)^3\ (1 - \beta_2)^3} \tag{7a}$$

$$= D_1\ (4\ \beta_1\ \beta_2\ \beta_3)\ G_s \tag{7b}$$

where

$$G_s = \frac{Z\ N\ K}{2\ \mu_a^2\ L_2\ (1 - \beta_1)^3\ (1 - \beta_2)^3} \tag{7c}$$

and where Z = number of electrons per atom of the scattering material

N = number of atoms per unit volume of the scattering material

$K = K(\theta_s, E_o)$ is the Klein-Nishina coefficient for scattering probability per electron (see Apprendix II for detailed definition of this term and its arguments - also note Figure 3 and Table IV)

$$\theta_s = 90^\circ - \alpha_1 - \alpha_2$$

$$\alpha_1 = \tan^{-1} \frac{W_1}{2 L_1 (1 - \beta_2)}$$

$$\alpha_2 = \tan^{-1} \frac{W_2}{2 L_2 (1 - \beta_1)}$$

From Figure 3 one can obtain the value of K/r_o^2 for various values of θ_s and E_o. From Table IV one can obtain appropriate values of $Z N r_o^2/\mu_a^2$. The multiplication of corresponding values of these two factors will give values for $Z N K/\mu_a^2$. (The factor r_o^2 drops out of the final expression as superfluous; it is included herein for reasons related to the basic derivation. The meaning of r_o is "the classical radius of the electron"; its value is about 2.8×10^{-13} cm.) The geometrical significance of α_1 and α_2 is indicated in Figure 15 of Appendix II.

We see from Equations 7 that dimensional scaling has the same effect on this contribution as it has on the contribution of the corner lip transmission effect, so all the corner lip effects scale in similar fashion, which, as we have pointed out, is not the same as for the basic effect of the prime scattering surfaces.

It also is to be noted that the contribution of this effect is roughly inversely proportional to the value of μ_a, and therefore decreases with increasing atomic numbers in much the same way as in the corner lip transmission effect. (Since μ_a is roughly proportional to NZ, one of the two factors in the μ_a^2 term in the denominator is cancelled in the proportionality calculation.)

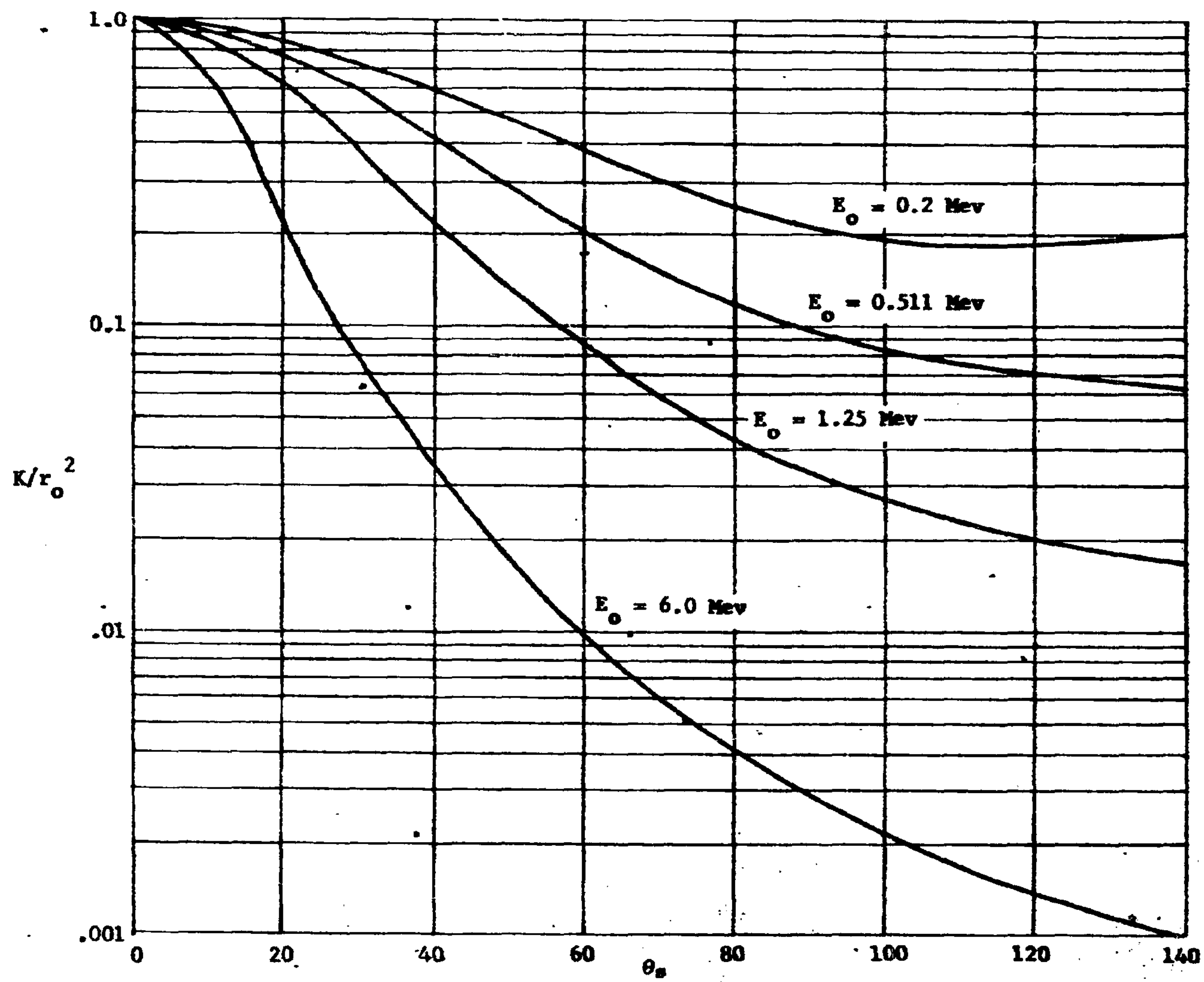

Figure 3. Klein-Nishina coefficient for scattering probability per electron.

IV. SUMMARY OF METHOD OF ANALYTICAL CALCULATIONS

A. Attenuation Factors

We are now at the point of being able to summarize the analytical formulas derived up to this point, with the hope that answers obtained for common situations meeting the qualifications given in Section II.B will be reasonably correct, at least for gamma rays.

Adding Equations 3, 6a, and 7b, we get the total dose at the end of the second leg:

$$D_{TOT} = D_1 \; (4 \; \beta_1 \; \beta_2 \; \beta_3) \; G_{TOT} \tag{8a}$$

where

$$G_{TOT} = G_b + G_t + G_s \tag{8b}$$

We are now at the point where we can introduce the attenuation factor and solve for it. For the purpose of this paper, we will use the following definitions:

$F_T = D_T/D_o$, being the ratio of dose at the end of the second leg to that at the reference point, one foot from the source in a nonabsorptive, nonscattering medium

$F_1 = D_1/D_o$, being the ratio of the dose at the intersection of the leg center lines to that at the reference point, one foot from the source in a nonabsorptive, nonscattering medium

$F_2 = D_T/D_1$, being the ratio of the dose at the end of the second leg to that at the intersection of the leg center lines

We will commonly call F_1 the attenuation factor for the first leg, and F_2 the attenuation factor for the second leg. Obviously, $F_T = F_1 \; F_2$.

We now find it possible to consider the attenuation factors for the two legs separately. We readily see that :

$$F_1 = \frac{1}{L_1^{\,2}} \tag{9}$$

and that

$$F_2 = 4 \; \beta_1 \; \beta_2 \; \beta_3 \; G_{TOT} \tag{10}$$

It is pointed out that in our discussion of model scaling relationships in Sections II.C, III.B, and III.C, the discussion was relative to the second-leg attenuation only, since the factors involving first-leg attenuation were eliminated from consideration.

By separating our factors in this way, we also allow ourselves, if we wish, to use a different reference point for overall attenuation (rather than the point at which D_o is measured) without affecting the analysis for F_2, which is the more difficult part.

B. Format and Data for Calculations

Tables V(a) and V(b) are a format which will permit ready calculation for this type of problem, using the information and formulas provided. Since F_1 is readily calculable, the forms are designed for the purpose of calculating F_2.

Since, at the present state of the art, precise knowledge of directional albedo is usually lacking, whereas, on the other hand, total albedo information is more generally available (Refs. 3, 4, and 5), some sort of assumption about directional distribution must be made. The forms are drawn up to permit use of the isotropic assumption. It is readily determined (see Equation 2b) that under the isotropic assumption the differential albedo equals the total albedo divided by 2π. Values for concrete and low-energy photons are given in Figure 4.

Table IV gives other various tabulated information needed in the solution of this problem, for various given energies. The energies used as arguments are selected for the following reasons: 6.0 Mev represents the energy of the most penetrating (and frequently the most abundant) photons in the initial radiation from nuclear weapons explosions in air. 1.25 Mev is the average energy for cobalt-60 gamma radiation, often used for experimental work; it is also a convenient energy to use to analyze fallout radiation problems. 0.5 Mev is close to the value of photon energies after a 90-degree Compton scattering, for incident gamma energies of general interest; also it is the approximate energy of positron annihilation radiation, which contributes heavily to the albedo from 6-Mev incident rays.

It might be pointed out that the data are not highly sensitive over wide regions to precise photon energies. For example, the energy absorption coefficient for most materials is fairly constant from 4 to 10 Mev, and thus the data for 6 Mev can be used for such cases. This coefficient is also quite constant for concrete and earth from 0.2 to 0.6 Mev, hence the use of 0.5 Mev as representative of scattered radiation energy is sufficiently accurate.

Table V(a). Form for Dose Computation

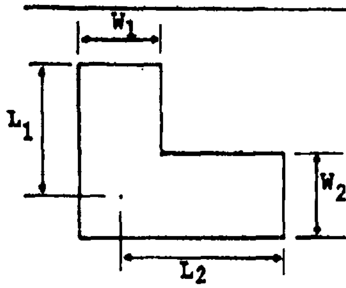

$^*L_1$ = ______ cm

L_2 = ______ cm

W_1 = ______ cm

W_2 = ______ cm

H = ______ cm

$\beta_1 = \frac{W_1}{2\,L_2}$

$\beta_2 = \frac{W_2}{2\,L_1}$

$\beta_3 = \frac{H}{2\,L_2}$

β_1 = ______

β_2 = ______

β_3 = ______

	$1 + \beta$	$1 - \beta$	$(1 - \beta)^2$	$(1 - \beta)^3$
β_1				
β_2				

Source Energy, E_o = ______ Mev

Scatt. Area	$\cos\theta_1$	
	Formula	Value
1	$\frac{W_1}{2\,L_1}$	
2	1.00	1.00
3	$\frac{H}{2\,L_1}$	
4	$\frac{H}{2\,L_1}$	
5	$\frac{W_1}{2\,L_1\,(1 - \beta_2)}$	
6	1.00	1.00
7	$\frac{H}{2\,L_1\,(1 - \beta_2)}$	
8	$\frac{H}{2\,L_1}$	

Enter curves (Fig. 4) for values of a_i using arguments of E_o and $\cos\theta_i$

a_1= ______

a_2= ______

a_3= ______

a_4= ______

a_5= ______

a_6= ______

a_7= ______

a_8= ______

*See footnote, Table V(b).

Table V(b). **Form for Dose Computation**

$G_b = \dfrac{a_1}{1+\beta_1} + \dfrac{a_2}{\beta_2\,(1+\beta_2)} + \dfrac{a_3}{1-\beta_1} + \dfrac{a_4}{1-\beta_2}$	
$= (\_\_\_) + (\_\_\_\_\_\_) + (\_\_\_) + (\_\_\_)$	$G_b =$ ________
* $G_t = \dfrac{(1-\beta_1)\,a_5 + 2\,a_7}{2\,\mu_a'\,L_2\,(1-\beta_1)^2\,(1-\beta_2)^3}$	
$+ \dfrac{(1-\beta_2)\,a_6 + 2\,\beta_2\,a_8}{2\,\mu_a\,L_1\,\beta_2(1-\beta_1)^2\,(1-\beta_2)^2}$	
$= \dfrac{(\_\_\_\_\_\_)}{(\_\_\_\_\_\_)} + \dfrac{(\_\_\_\_\_\_)}{(\_\_\_\_\_\_)}$	
$= (\_\_\_\_\_\_) + (\_\_\_\_\_\_)$	$G_t =$ ________
* $G_s = \left(\dfrac{Z\,N\,K}{\mu_a^2}\right)\left(\dfrac{1}{2\,L_2\,(1-\beta_1)^3\,(1-\beta_2)^3}\right)$	$G_s =$ ________
$F_2 = 4\,\beta_1\,\beta_2\,\beta_3\,G_{TOT}$	$G_{TOT} =$ ________
$D_1 =$ ________	$F_2 =$ ________
Dose $= D_1\,F_2$	Dose = ________

* Note: Use of Table IV requires all lengths to be measured in centimeters, all values of linear absorption coefficient to be in reciprocal centimeters.

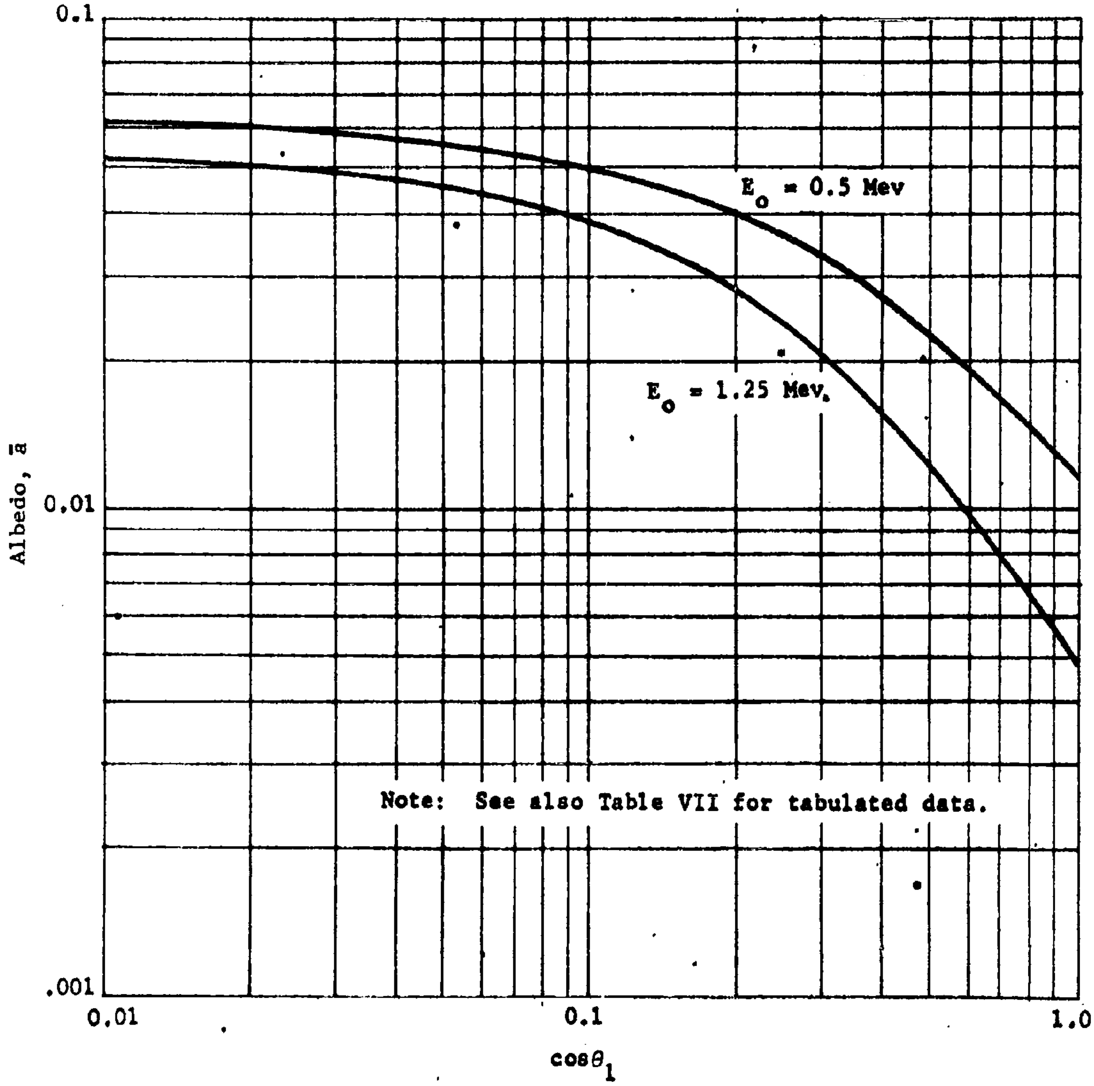

Figure 4: Differential, directional dose - bedo for 1.25 and 0.5 Mev gamma photons from concrete (isotropic assumption).

Table VII. Differential Directional Dose Albedo for Gamma Rays Scattered From Concrete (Isotropic Assumption)

$Cos\theta_1$	E_o = 0.5 (Mev)	E_o = 1.25 (Mev)
0.01	.0628	.0522
0.02	.0588	.0509
0.03	.0572	.0493
0.04	.0552	.0469
0.05	.0547	.0453
0.06	.0530	.0437
0.07	.0518	.0424
0.08	.0517	.0413
0.09	.0495	.0402
0.10	.0491	.0390
0.20	.0394	.0287
0.30	.0326	.0218
0.40	.0275	.0186
0.50	.0232	.0130
0.60	.0189	.0105
0.70	.0164	.00843
0.80	.0146	.00684
0.90	.0132	.00588
1.00	.0118	.00508

V. TECHNIQUES FOR HANDLING CERTAIN COMPLICATIONS AND VARIATIONS

A. General Comment

There are certain considerations in the above formulation which have been slighted, for the sake of avoiding too great a degree of elaboration and because adequate techniques for handling them to the desired degree of accuracy are not readily available at present. Under certain circumstances, however, they may become somewhat significant, providing correction factors in excess of 10 percent. Likewise, if we encounter problems in which the given conditions and physical parameters do not meet those specified in Section II.B, certain changes in the approaches may be desirable.

Even though some of these modifications may be difficult to handle analytically to the desired precision, we can give some recommendations as to how they can be appropriately accomplished, at least approximately.

B. Variation in Source Configuration

In practical cases it is unlikely that one will be dealing with a source concentrated at the center of the entrance to the duct system. One is much more likely to find the source distributed over the entrance or to find the radiation streaming in from outside. If such radiation passes down the first leg in an approximately symmetrical way, one might expect the foregoing analysis to be generally valid as regards the scattering from the corner walls and the corner lip effects. We would expect the previously derived formulas for F_2 to be reasonably valid in such case.

On the other hand, the value for F_1 may be rather strongly dependent upon the character of the source at the entrance, for two reasons: The angular distribution of the incoming radiation may not be such as to lead to a simple inverse-square relationship of dose rate with distance; and a more appropriate reference point may be necessary or desirable as the basis for the attenuation factor down the first leg.

The question arises, then, for each source situation: What is the value of the dose rate at a distrance L_1 along a rectangular tunnel, or hole, as compared with the dose rate at the entrance or at some other appropriate reference point? The following subsections discuss some of the more important of these situations.

1. Distributed source at duct entrance

In this type of source we assume that the radiation source is at the entrance of the duct, but is equally distributed across it. This is what is normally called the "isotropic" case (Ref. 6, Sect. 4.12). In this case the readings down the first leg are proportional to $\ln(1 + W_1 H/\pi x^2)$, provided the width and height of the first leg do not differ too radically in amount. Then the attenuation factor F_1 depends on what is used as the reference point. If the reference point is taken as one unit of distance away from the center of the entrance face of the duct, the first leg attenuation factor becomes, approximately:

$$F_1' \cong \frac{W_1 H}{\pi L_1^2 \ln\left(1 + \frac{W_1 H}{\pi}\right)} \tag{11}$$

since $\ln(1 + W_1 H/\pi L_1^2)$ approaches $W_1 H/\pi L_1^2$ for an argument much greater than unity.

If the reference point is taken as being three feet above a smooth, infinite plane, covered to the same amount per unit area with distributed radiation sources, emitting isotropically, one can show that (see Appendix III):

$$F_1'' \cong \frac{W_1 H}{34 L_1^2} \tag{12}$$

2. Cosine emission source

If the radiation crossing the plane of the duct entrance has an angular distribution such that the amount passing through the entrance from directions at various angles to the leg axis is proportional to the cosine of the direction line with the leg axis, the distribution is called "cosine." It is interesting to note that this situation can actually be created by a superposition of parallel, broad-beam radiation beams coming with equal intensity from each direction in toward the duct opening. It is thus, with respect to an isotropic instrument outside the duct entrance, isotropic; but as far as the amount penetrating the duct entrance, it is angle-dependent, since the amount penetrating depends on the angle of "aspect" of the entrance area to the radiation coming from a certain direction.

Under these circumstances, it may be shown that the attenuation factor in the first leg, based upon a reference value at or just outside the entrance to the duct, is (Ref. 6, par. 4.12):

$$F_1''' = \frac{W_1 H}{2\pi L_1^2} \tag{13}$$

provided the ratio between the first leg width and height does not vary too markedly from unity.

Under many general conditions, a crude approximation to the problem of initial nuclear weapon radiation entering a shelter entranceway may make use of this approach.

3. Other types of sources

The nature of the incoming source radiation, particularly its directional distribution, can make a great difference in the value of F_1. For example, monodirectional radiation coming in parallel to the axis of the first leg will reach a detector at the end of the first leg unattenuated. In such a case the value of F_1 is obviously unity. On the other hand, a monodirectional beam parallel to the entrance of the duct system will not enter at all, and the value of F_1 for this case is zero.

If the directional distribution of radiation coming from without is irregular, one may consider the proportion of the radiation coming in through a solid angle subtended by the entrance to the duct, as seen from the point of intersection of the two leg center lines, compared to the total coming from all directions to a detector on the outside. This proportion will give the proper value of F_1, based on the said outside reference point. The situation covered in Subsection 2, above, is a simple case for this situation. On the other hand, if the radiation is coming predominantly from one side, this approach cannot be used blindly. The major source of radiation down the first leg in such a case might well be that scattered off a wall just inside the entrance to the first leg.

C. Multiple Scattering from Duct Leg Walls

Hitherto, we have assumed that the radiation detected at the end of the first leg is that coming directly from or through the entrance to the duct; likewise we have assumed that the radiation reaching the detector at the end of the second leg is that with has been contributed only by reflection from surfaces A_1 through A_8, inclusive, plus that in-scattered by the corner lip. It is obvious, however, that such an assumption ignores the possibility of an appreciable contribution from duct leg walls outside those already designated as primary or lip-transmission scattering surfaces. The question arises: What error is involved in this assumption?

It must be confessed that under many circumstances within the assumptions of this paper there are probably situations in which the error involved in ignoring multiple scatter is greater than 10 percent.

Unfortunately, this subject has not been too well analyzed in the past, except for conditions in which the albedo scattering is independent of the incident angle and depends in very simple (isotropic or cosine) fashion upon the angle of emergence. Such an approach may be better for neutrons than gamma rays (see Refs. 1, 3, and 6), and furthermore it is dependent upon having good albedo information. Rough calculations and experimental data indicate that this effect may increase leg attenuation factors by well over 10 percent for gamma rays passing through concrete ducts (Ref. 3). (Note that by an increased attenuation factor we are indicating a poorer degree of attenuation.) Attenuation in the second leg may be more affected than in the first leg, since the albedo for light materials such as concrete increases as the energy is lowered (Refs. 4 and 5).

D. Direct Transmission Effect

For ducts of smaller size, it is possible that appreciable radiation may be transmitted directly from source to detector. The computation of this effect is quite straightforward. We cannot apply the results directly to the various attenuation factors, but must add doses or dose rates (absolute or relative).

From Figure 2 we readily see that the distance between the source and detector is $\sqrt{L_1^2 + L_2^2}$. However, the direct-line thickness of wall material is $(1 - \beta_1 - \beta_2)\sqrt{L_1^2 + L_2^2}$. (We assume the intervening material to be homogeneous — if not, appropriate modification to the analysis can be made.)

It appears suitable to use the build-up factor as determined for an ideal case in which source and detector are imbedded in infinite, homogeneous material (see Ref. 7). We thus conclude that:

$$D_d = \frac{D_o \, B \, \exp\left[\mu_o \, (1 - \beta_1 - \beta_2)\sqrt{L_1^{\,2} + L_2^{\,2}}\right]}{(1 - \beta_1 - \beta_2)^2 \, (L_1^{\,2} + L_2^{\,2})} \tag{14}$$

where μ_o is the total absorption coefficient for gamma rays of the initial energy at the source passing through the given duct wall material. The build-up factor, B, is a function of the number of mean free paths through the wall material. The number of mean free paths is equal to $\left[\mu_o \, (1 - \beta_1 - \beta_2)\sqrt{L_1^{\,2} + L_2^{\,2}}\right]$, and is obtained from Ref. 7, appropriate extracts from which are provided in Table VI.

Table VI. Dose Build-up Factors for Aluminum and Other Light Materials (From Ref. 7)

Photon Energy (Mev)	No. of Mean Free Paths						
	1	2	4	7	10	15	20
0.5	2.37	4.24	9.47	21.50	38.90	80.80	141.00
1.0	2.02	3.31	6.57	13.10	21.20	37.90	58.50
2.0	1.75	2.61	4.62	8.05	11.90	18.70	26.30
3.0	1.64	2.32	3.78	6.14	8.65	13.00	17.70
4.0	1.53	2.08	3.22	5.01	6.88	10.10	13.40
6.0	1.42	1.85	2.70	4.06	5.49	7.97	10.40

Note: The source is considered point-isotropic.

VI. COMPARISON WITH EXPERIMENT

C. Eisenhauer has performed some experiments with small concrete ducts and cobalt-60 (Ref. 8). Figure 5 is a comparison of Eisenhauer's experimental results and the LeDoux-Chilton analysis using the isotropic differential albedo assumption. Because of the assumptions made in Section II.B, correlation with experiments of small L/W ratios was not expected. Overall agreement is good.

In order to measure the effect of the corner contribution, Eisenhauer placed a lead block in the corner of the duct and then measured the remaining gamma dose. Figure 6 is a comparison of experimental data with the LeDoux-Chilton analysis for this case. In order to make the calculations for this case, the proper values for lead from Table III must be used in computing G_t and G_s, which are the contributions from the corner. Eisenhauer does not consider his data highly accurate, and the very close agreement is considered rather fortuitous under the circumstances.

Charles Terrell has performed experiments on large (6-ft by 6-ft) ducts (Ref. 3). Figure 7 is a comparison of the LeDoux-Chilton analysis with his results. Agreement is again good.

For these analytical comparisons, none of the complications discussed in Section V were allowed for.

From these comparisons it thus appears that a basic theoretical analysis can give results which check very well with experimental results. The isotropic distribution assumption for differential directional albedo seems to be an excellent choice. The effect of using more accurate albedo data awaits the publication of such data. Meanwhile, for the cases considered, the LeDoux-Chilton method of analysis appears to be sufficiently accurate for practical shielding computations. Data from Table VII may be used for practical shielding computations based on the isotropic albedo.

VII. NEED FOR FUTURE WORK

The Monte-Carlo calculations now being done (such as the work in progress by D. Raso of Technical Operations, Inc.) should yield sufficient data for the differential dose albedos for energies from 0.2 to over 10 Mev, for the materials of shielding importance. It is hoped that this work will permit a more accurate comparison of this analytical approach and experimental results.

More experimental data is needed for distributed sources, for other source energies, and for neutrons. Terrell, of Armour Research Foundation, is doing work in this direction. Once a good correlation is obtained it will be possible to analyze duct and entranceway shelter radiation streaming problems with adequate accuracy.

There is also the possibility of experimental analyses of even more complex situations through work with ducts of small scale.

ACKNOWLEDGEMENT

The need for further development of work along the line of radiation penetration through ducts and entranceways which we are attempting to fulfill in part here was recognized as a result of a number of experimental efforts in the nuclear defense field by various workers. This work has been especially stimulated by the work of Eisenhauer of the National Bureau of Standards (Ref. 8). Fruitful discussions on these matters with Eisenhauer and Berger of the National Bureau of Standards, Terrell of Armour Research Foundation, and their associates are appreciatively acknowledged.

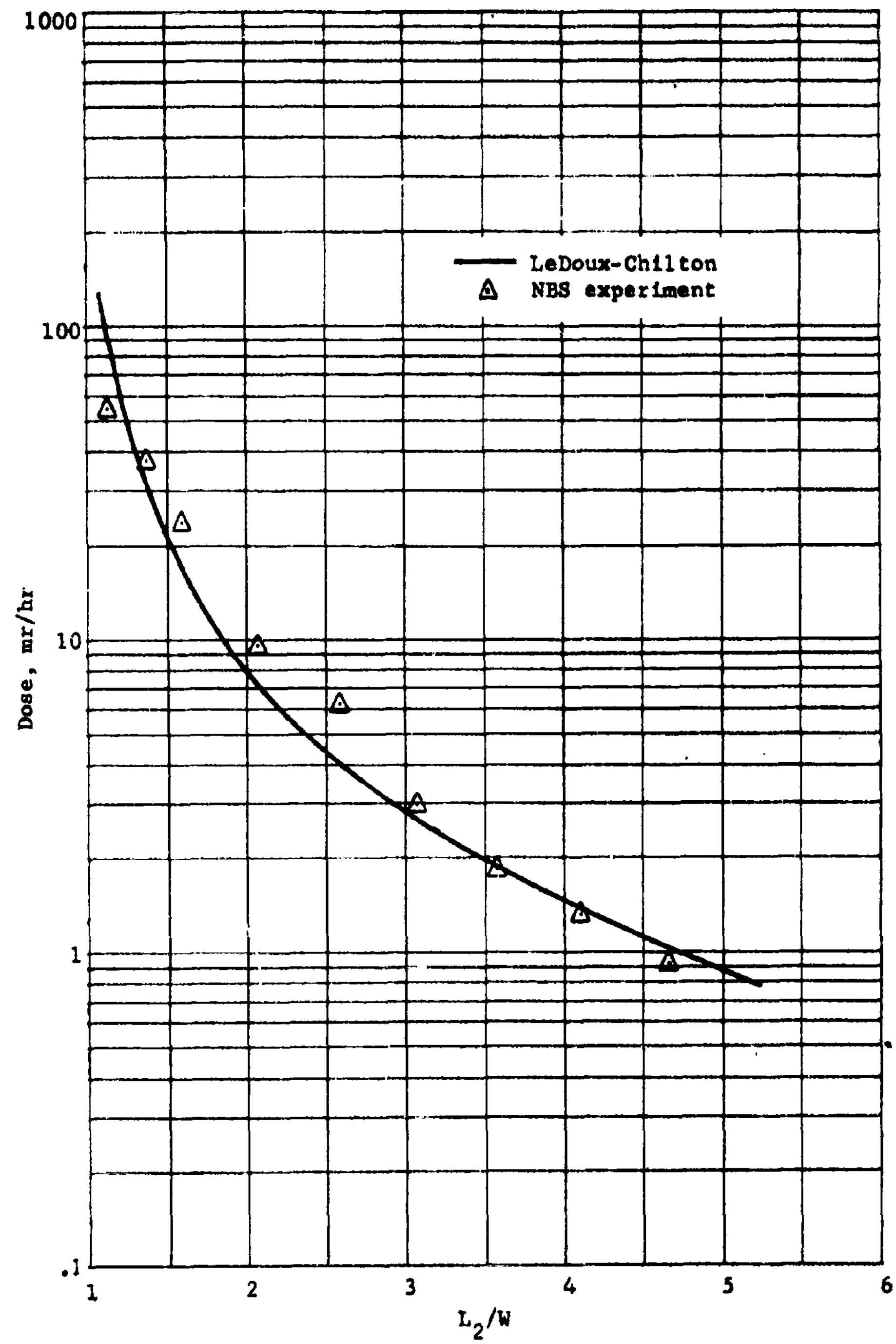

Figure 5. Comparison of LeDoux-Chilton analysis with NBS experiment using cobalt-60 and a concrete duct, W = 19.2 cm.

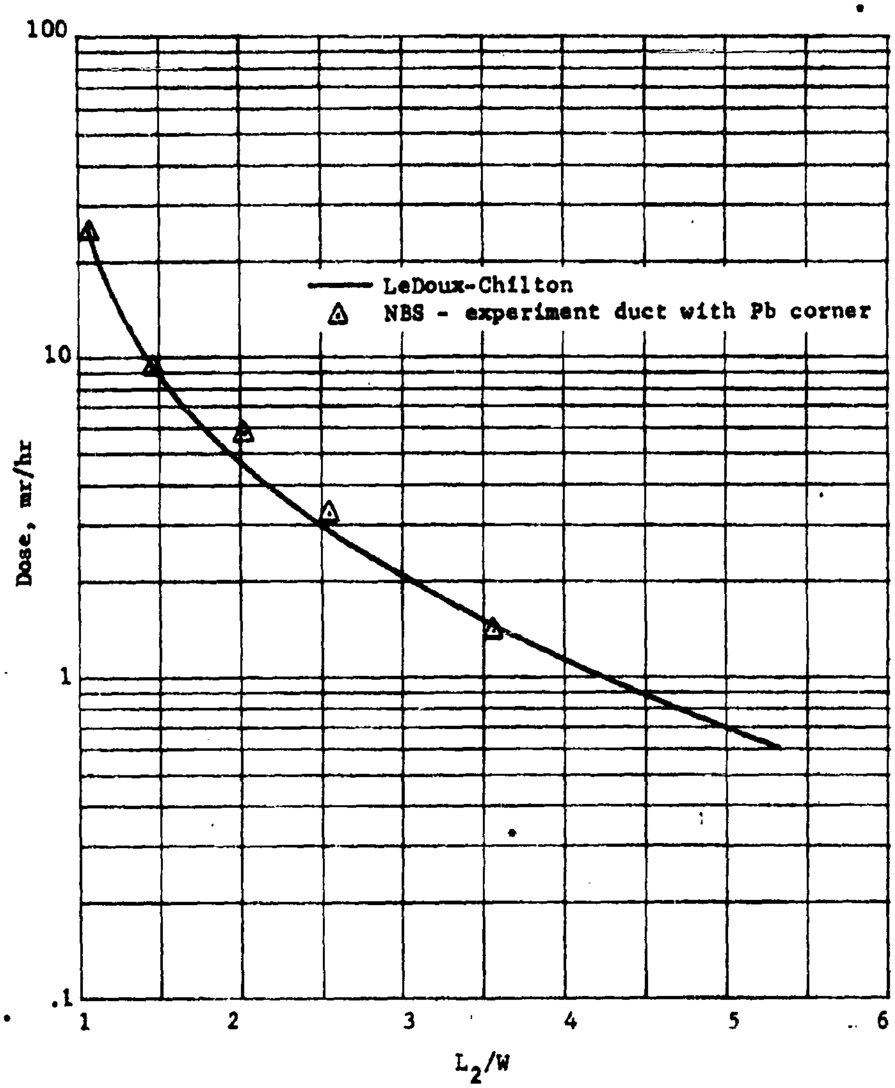

Figure 6. Comparison of the LeDoux-Chilton analysis with NBS experiment using cobalt-60 and a concrete duct with lead corner lip, W = 19.2 cm.

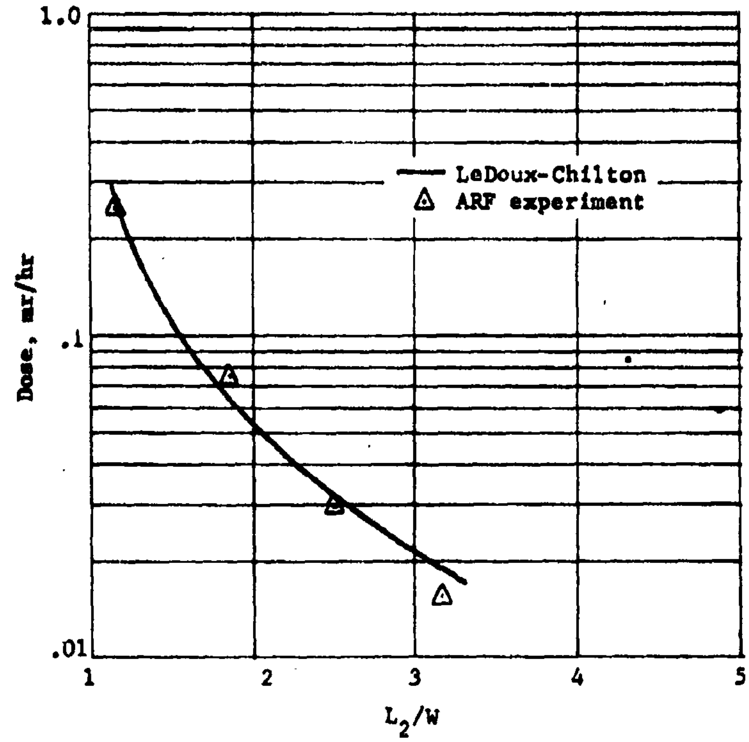

Figure 7. Comparison of the LeDoux-Chilton analysis with ARF experiment using cobalt-60 and a concrete duct, W = 6 feet.

REFERENCES

1. Rockwell, T., III, editor. "Reactor Shielding Design Manual," Chapter 8, USAEC Doc. TID-7004. Off. of Tech. Serv., Dept. of Commerce (1956).

2. Heitler, W. "The Quantum Theory of Radiation," Second Ed., Oxford Press (1944).

3. Terrell, C. W., et al. "Radiation Streaming in Shelter Entranceways," Armour Res. Fdn. Rpt. ARF 1158-12 (1960).

4. Berger, M., and D. Raso. "Backscattering of Gamma Rays," NBS Rpt. 5982 (1958). Also published in Radiation Research, 12, 20-37 (1960).

5. Perkins, J. F. "Monte Carlo Calculation of Gamma-Ray Albedo of Concrete and Aluminum," Jour. Appl. Physics, 16, No. 4 (June 1955).

6. Price, B. T., et al. "Radiation Shielding," Pergamon Press (1957).

7. Goldstein, H., and J. E. Wilkins, Jr. "Calculations of the Penetration of Gamma Rays," U. S. Atomic Energy Comm. Doc. NYO-3075. Supt. of Doc., U. S. Govt. Print. Off. (1954).

8. Eisenhauer, C. "Scattering of Cobalt-60 Gamma Radiation in Air Ducts," NBS Tech. Note 74 (1960).

9. Donovan, L. K. and A. B. Chilton. "Dose Attenuation Factors for Concrete Slab Shields Covered with Fallout as a Function of Time after Fission." (To be published as NCEL Tech. Rpt. R-137).

10. Berger, M. J., and L. V. Spencer. "Penetration of Gamma Rays from Isotropic Sources through Aluminum and Concrete," NBS Tech. Note 11 (1959).

11. LeDoux, J. C., and L. K. Donovan. "Compilation of Exponential Functions for Arguments from 2 through 50," U. S. Naval Civ. Eng. Lab. Tech. Comp. C-003 (1960).

Appendix I

CORNER LIP TRANSMISSION EFFECT

The case to be considered is a rectangular duct as shown in Figure 8. The height of the duct is H, the dimension perpendicular to the plane of the paper. It is not reasonable to assume different heights of the two duct legs, since the simplest way of joining the duct legs is to require a common height H. The widths of the ducts are W_1 and W_2. We will consider a general case of nonperpendicular duct legs, and will particularize to the perpendicular case later.

Figure 9 illustrates the geometry of the corner lip transmission effect for the ray which is transmitted through the lip prior to being reflected off a duct wall. For convenience, this effect will hereinafter be called simply the "transmission effect." The duct has legs of lengths L_1 and L_2, intersecting at an angle δ. We consider a photon from the source S which traverses the corner through a thickness before being reflected from Leg 2 into the detector.

If we focus our attention on the corner lip itself, Figure 10, it can be seen that there is approximately a parallel beam of photons striking the corner at an angle α_1 (assuming $L_1 \gg W_1$). If the intensity striking the corner is I(mev/cm^2), and the thickness of the beam is dx, then the total energy per unit height of the duct would be I dx. Because of absorption within the material, the total energy per unit height and beam thickness dx, emerging from the corner would be $I\ e^{-\mu y}\ dx$. Since a small scattering angle and multiple scattering may in part still provide photons in the direction of interest, only the net energy absorptions should be considered. Hence, the μ we recommend to be used here is μ_a, the linear energy absorption coefficient, closely equivalent to the "effective" absorption coefficient.

Since only the gamma rays which emerge from the corner lip with no (or almost no) interaction are of interest, we could replace the actual situation depicted in Figure 10 with an equivalent transparent corner as shown in Figure 11. This "equivalent lip" is characterized by a dimension T_2 such that the amount of photon energy which is transmitted by this truncated lip is the same as that transmitted through the actual lip. It is assumed, in the equivalent case, that any photons which strike the lip material so as to seem to pass beyond T_2 are totally absorbed.

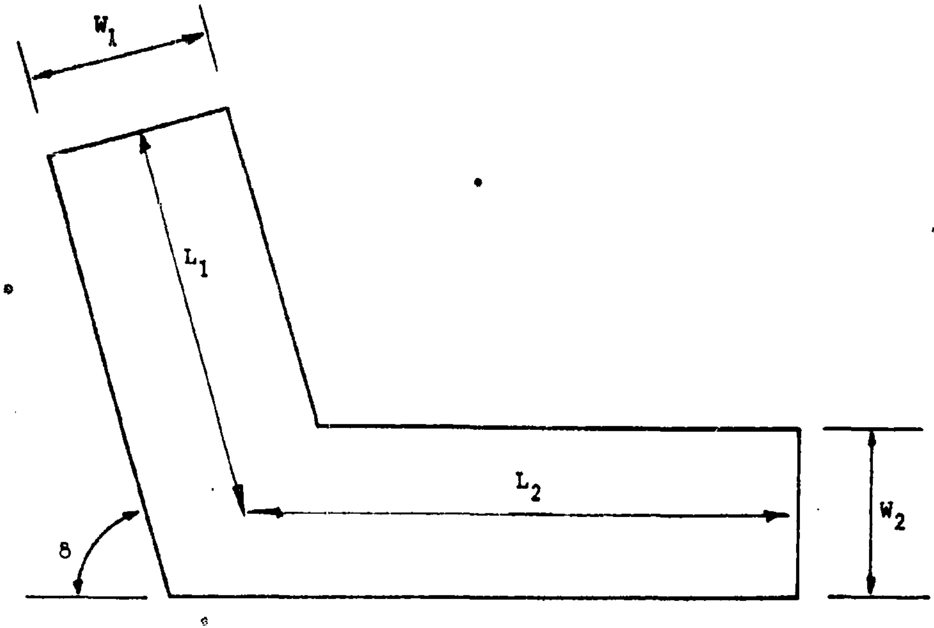

Figure 8. A rectangular duct with common height H of widths W_1 and W_2, lengths L_1 and L_2 intersecting at the angle δ.

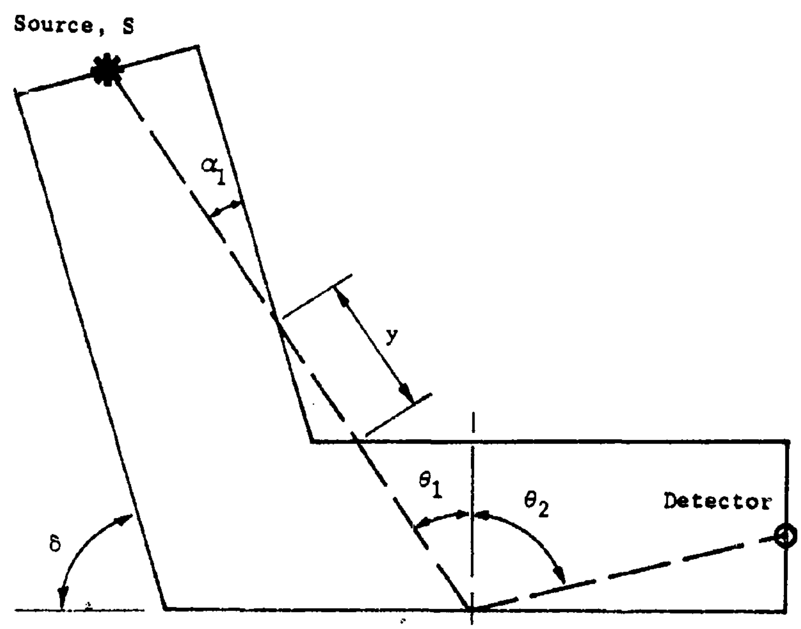

Figure 9. Geometry for corner lip transmission effect——ray from source side.

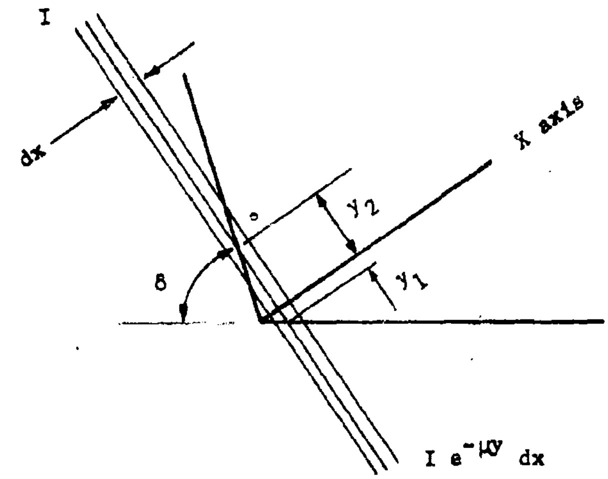

Figure 10. Attenuation of gamma flux I through corner.

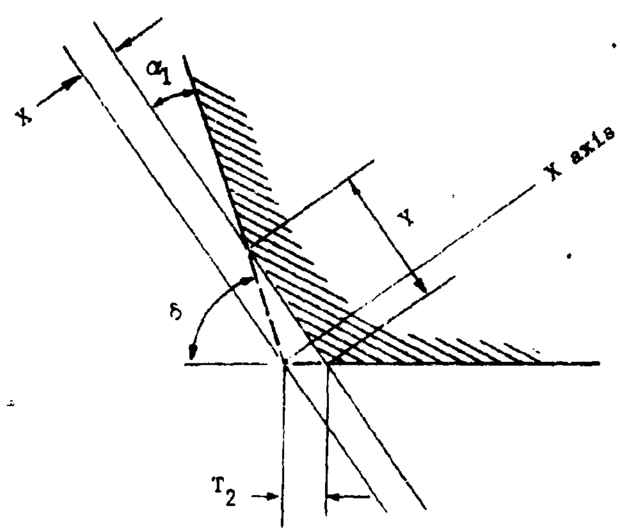

Figure 11. Equivalent transparent corner for transmission effect.

Mathematically this can be expressed by the following equation:

$$\int_{0}^{\infty} I\, e^{-\mu_a y}\, dx = \int_{0}^{X} I\, dx \qquad \text{(I-1)}$$

From Figure 10:

$$y = x \cot(\delta-\alpha_1) + x \cot\alpha_1 \qquad \text{(I-2)}$$

where x is the distance from the corner to the path of the photon.

The results of integrating Equation I-1 are:

$$X = \frac{1}{\mu_a \left[\cot\alpha_1 + \cot(\delta-\alpha_1)\right]} \qquad \text{(I-3)}$$

From Figure 11:

$$X = T_2 \sin(\delta-\alpha_1) \qquad \text{(I-4)}$$

Combining Equations I-3 and I-4, the lip dimension T_2 is:

$$T_2 = \frac{\sin\alpha_1}{\mu_a \sin\delta} \qquad \text{(I-5)}$$

In a similar fashion the dimension of the lip along leg 1 for the ray which strikes the wall of leg 1 first and then penetrates the lip is:

$$T_1 = \frac{\sin\alpha_2}{\mu_a \sin\delta} \qquad \text{(I-6)}$$

From the figures it can be seen that μ_a depends on E_o, the energy of the source, and μ_a' depends on E_1, the energy after reflection from the walls of the first leg of the duct.

Using the values of T_1 and T_2, the various values of parameters needed for computation of the dose from these transmission areas can be computed and are listed in Tables I and II in the main text. It should be remembered that the assumption of $L \gg W$ still holds. This is equivalent to saying that $\sin\alpha \cong \tan\alpha$.

If δ is 90 degrees, then T_1 and T_2 can be particularized as follows:

$$T_1(90^o) = \frac{\sin\alpha_2}{\mu_a'} \qquad \text{(I-7)}$$

$$T_2(90^o) = \frac{\sin\alpha_1}{\mu_a} \qquad \text{(I-8)}$$

It is readily demonstrated that the value of Y in Figure 11 equals $1/\mu_a$, the "effective" mean free path for energy transmission.

Application of these results to dose measurements makes use of the fact that, within broad energy limits, dose is approximately proportional to energy flux.

Appendix II

IN-SCATTERING CORNER LIP EFFECT

Figure 12 illustrates the geometry considerations in the "in-scattering corner lip effect analysis" (hereinafter termed the "in-scatter effect").

The photons are assumed to strike the corner in an essentially parallel beam, perpendicular to the lip height. This is believed to be a valid assumption for $L/W \geq 3$ and for a small scattering volume.

Let us consider a photon striking at point B, suffering a scattering collision at B and then traveling along line BA to the detector. If we define a distance y by letting AB = y, we will concern ourselves for the moment with all other photons which travel the same distance y within the corner lip material and reach the detector. The other extreme would be a photon traveling along DC from the source and scattering just at C into the detector such that CD = AB = y. The rays are essentially parallel on entering or leaving the corner.

Suppose we now take any other photon traveling along a path FG-GE which has a scattering collision along the straight line CB and is scattered in a direction parallel to the first two photon exit directions. Will it also have the same distance of travel in the lip material? If so, we can then analyze a small volume element along the line CB and then integrate over all volume elements (have all path lengths) to determine the total single scattering contribution from the corner.

In Figure 12 we are given that AB = CD = y. The entering and exit rays are parallel. The problem is to prove that CD is a locus of all scattering points which provide the lip travel distance Y for all rays having entrance and exit directions indicated.

$$\triangle ABC \sim \triangle EGC \tag{II-1}$$

$$\triangle CDB \sim \triangle GBF \tag{II-2}$$

Therefore,

$$\frac{EG}{AB} = \frac{CG}{CB} \tag{II-3}$$

and

$$\frac{GF}{CD} = \frac{GB}{CB} \tag{II-4}$$

But $$CB = CG + GB \tag{II-5}$$

Therefore, $$EG = \frac{(AB)\ (CG)}{CG + GB} \tag{II-6}$$

and $$GF = \frac{(CD)\ (GB)}{CG + GB} \tag{II-7}$$

But $$AB = CD = y \tag{II-8}$$

Therefore, $$EG + GF = \frac{y\ (CG)}{CG + GB} + \frac{y\ (GB)}{CG + GB} \tag{II-9}$$

Thus $$EG + GF = y \tag{II-10}$$

It can be shown that no point off the line CB has the desired property. Therefore CB is the stated locus, which was to be proved.

Reconstructing Figure 12 to indicate the principal quantities, we have Figure 13, from which the following identities are obtained:

$$OC = \frac{y \sin\alpha_1}{\sin\delta} \tag{II-11}$$

$$OD = \frac{y \sin(\delta-\alpha_1)}{\sin\delta} \tag{II-12}$$

$$OB = \frac{y \sin\alpha_2}{\sin\delta} \tag{II-13}$$

$$OA = \frac{y \sin(\delta-\alpha_2)}{\sin\delta} \tag{II-14}$$

$$CB = \left[\cot\psi + \cot(\delta-\psi)\right] x \tag{II-15}$$

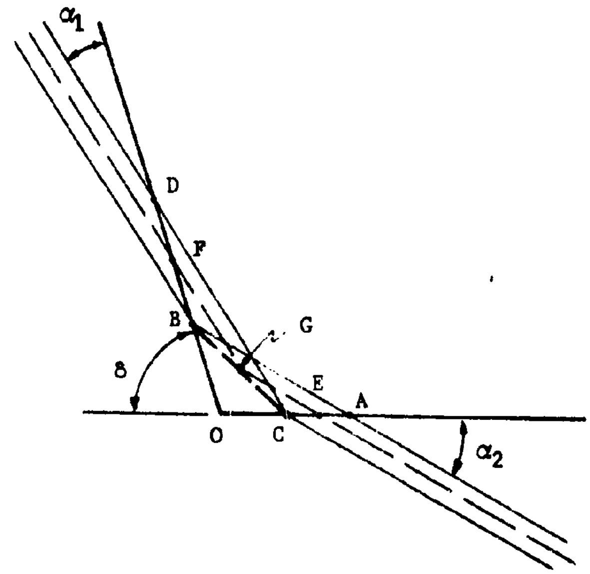

Figure 12. Geometry for in-scattering corner effect.

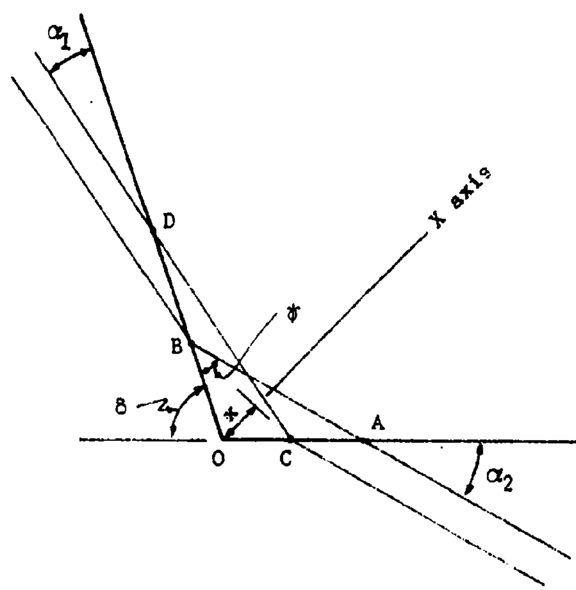

Figure 13. Simplified Figure 12.

$$\text{or} \qquad CB = hx \tag{II-16a}$$

$$\text{where} \qquad h = \left[\cot\psi + \cot(\delta - \psi)\right] \tag{II-16b}$$

From ΔOCB:

$$(CB)^2 = (OC)^2 + (OB)^2 + 2\,(OC)\,(OB)\cos\delta \tag{II-17a}$$

$$= \frac{y^2}{\sin^2}\left[\sin^2\alpha_1 + \sin^2\alpha_2 + 2\sin\alpha_1\,\sin\alpha_2\,\cos\delta\right] \tag{II-17b}$$

$$\text{or} \qquad CB = \frac{y\,J}{\sin\delta} \tag{II-18a}$$

$$\text{where} \qquad J = \left[\sin^2\alpha_1 + \sin^2\alpha_2 + 2\sin\alpha_1\,\sin\alpha_2\,\cos\delta\right] \tag{II-18b}$$

Therefore, from Equations II-16a and II-18a,

$$\frac{y\,J}{\sin\delta} = hx \tag{II-19}$$

$$\text{and} \qquad y = \frac{x\,h\,\sin\delta}{J} \tag{II-20}$$

$$\text{or} \qquad y = m\,x \tag{II-21}$$

$$\text{where} \qquad m = \frac{h\,\sin\delta}{J} \tag{II-22}$$

Since m is a function of the various duct angles, it can be considered as a constant in any specific case.

With the basic quantities defined we can now proceed to determine the in-scattering caused by the corner lip. Figure 14 illustrates a differential volume dV, which is equal to the thickness dx times the height of the duct H times the length CB, or

$$dV = (CB)\ H\ dx \qquad \text{(II-23)}$$

But $$CB = h\ x \qquad \text{(II-16a)}$$

Therefore, $$dV = H\ h\ x\ dx \qquad \text{(II-24)}$$

The number of electrons per unit volume is NZ, where N is the number of atoms per cc and Z is the number of electrons per atom. The number of scatterers in volume element $dV = N\ Z\ H\ h\ x\ dx$. (II-25)

If I_o is the intensity at unit distance from the source S, then the intensity at the differential volume would be $I_o/R_1{}^2$, where R_1 is the distance from the source to the scattering volume. The differential intensity dI at the detector from volume dV would then be:

$$dI = \frac{I_o\ N\ Z\ H\ h\ K(\theta,E_o)\ x\ e^{-\mu m x}\ dx}{R_1{}^2\ R_2{}^2} \qquad \text{(II-26)}$$

where $e^{-\mu m x}$ is the probability of a photon not being absorbed or otherwise eliminated from an accepted path

$K(\theta,E_o)$ is the probability of an amount of energy being scattered through the appropriate angle into the detector, if initial photons have a monoenergetic value of E_o (Klein-Nishina Scattering Probability)

R_2 is the distance from dV to the detector

$$K(\theta_1, E_o) = \frac{r_o^2 (1 + \cos^2\theta)}{2\left[1 + \gamma_o (1 - \cos\theta)\right]^3} \left\{ 1 + \frac{\gamma_o^2 (1 - \cos\theta)^2}{(1 + \cos^2\theta)\left[1 + \gamma_o (1 - \cos\theta)\right]} \right\} \qquad \text{(II-27)}$$

where r_o is the "classical" radius of the electron ($r_o^2 = 7.9403 \times 10^{-26}$ cm^2)

θ is the angle of scatter and equals $\delta - \alpha_1 - \alpha_2$ (II-28)

γ_o is the photon energy in terms of the self-energy of the electron and equals E_o(Mev)/0.511 (II-29)

For practical purposes, $\frac{I}{I_o} = \frac{D}{D_o}$. Then by integrating, we find:

$$D = \frac{D_o\, N\, Z\, H\, h\, K}{R_1^2\, R_2^2} \int_o^\infty x\, e^{-\mu m x}\, dx \qquad \text{(II-30)}$$

or

$$D = \frac{D_o\, N\, Z\, H\, h\, K}{R_1^2\, R_2^2\, (\mu m)^2} \qquad \text{(II-31)}$$

The volume which will contribute largely to the in-scattering effect will be small for practical cases. Figure 15 depicts the various quantities required to solve for D. α_1 and α_2 are the same angles as in the transmission corner effect (see Appendix I). From Figure 15,

$$R_1 = \frac{W_1}{2 \sin\alpha_1} \qquad \text{(II-32)}$$

$$R_2 = \frac{W_2}{2 \sin\alpha_2} \qquad \text{(II-33)}$$

As in previous cases, we will use μ_a for μ.

From the geometry of the duct it can be shown that:

$$\frac{h}{m^2} = \frac{\sin\alpha_1 \sin\alpha_2}{\sin\delta} \qquad \text{(II-34)}$$

Making this substitution, Equation 3 becomes:

$$D = \frac{D_o\ Z\ N\ K\ H \sin\alpha_1 \sin\alpha_2}{\mu_a^2\ R_1^2\ R_2^2 \sin\delta} \qquad \text{(II-35)}$$

With the assumption that $\sin\alpha \cong \tan\alpha$, and substituting the proper functions into Equation 4, the final form for the dose contribution from in-scattering in the corner for $\delta = 90^\circ$ would be:

$$D_s = D_1 \left(\frac{W_1\ W_2\ H}{2\ L_1\ L_2^2}\right)\left[\frac{Z\ N\ K}{2\ \mu_a^2\ (1 - \beta_1)^3 (1 - \beta_2)^3}\right] \qquad \text{(II-36)}$$

Table IV contains values of $r_o^2\ Z\ N/\mu_a^2$ for various gamma energies and materials. For obtaining values for K/r_o^2, use Figure 3. Assuming a small scattering volume, the value of θ which should be used for entry into Figure 3 would be:

$$\theta_s = \delta - \alpha_1 - \alpha_2 \qquad \text{(II-28)}$$

$$\alpha_1 = \tan^{-1} \frac{W_1}{2\ L_1\ (1 - \beta_2)} \qquad \text{(II-37)}$$

$$\alpha_2 = \tan^{-1} \frac{W_2}{2\ L_2\ (1 - \beta_1)} \qquad \text{(II-38)}$$

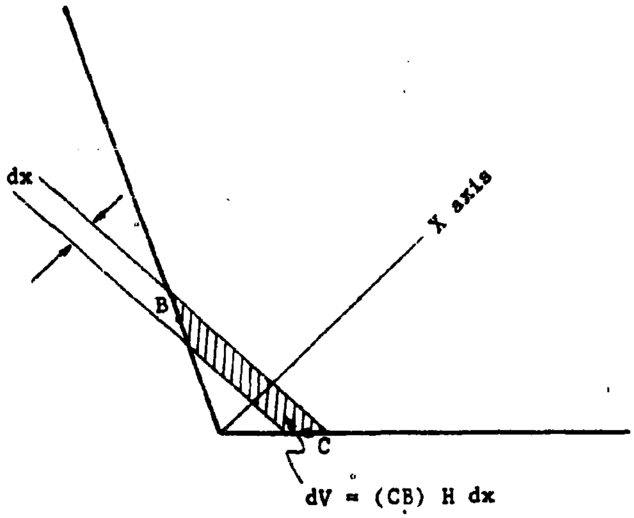

Figure 14. Differential volume of the in-scattering corner effect.

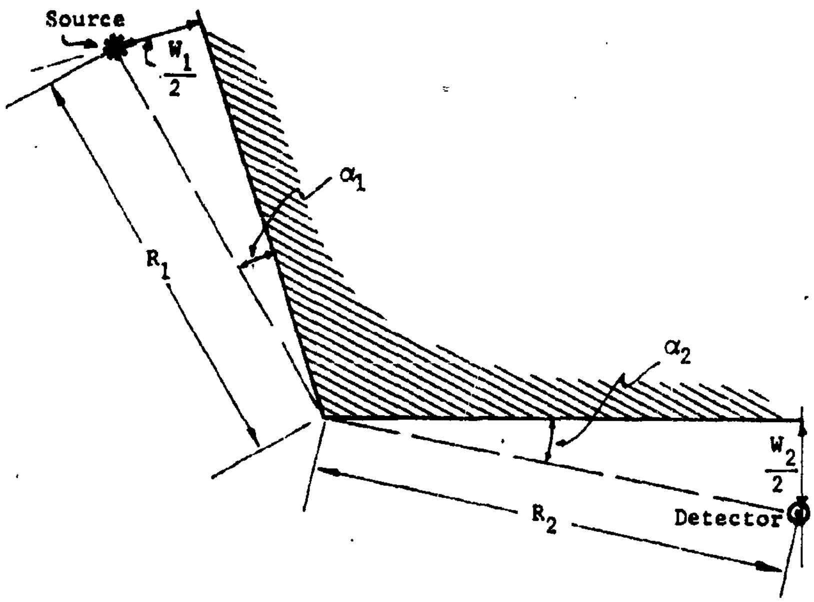

Figure 15. Simplified geometry as applied to in-scattering corner effect.

ERRATA

TECHNICAL NOTE TN-383

PAGE 10, Table III
In the formula for Dose Contribution for Area #4, the subscript for the "β" should be 2 rather than 1

PAGE 15, Table IV
In the Note #1, the "μ" should have subscript "a" on it.
In Note #2, first line, the word "inversely" should be "directly".
The last line of Note #2, should be changed to read as follows. "The term

$$\left(\frac{Z\,N}{\mu_a^{2}}\right)_a^{2}$$

is inversely proportional to density if the average atomic number is the same."

PAGE 42, Equation 4-36
The factor within the brackets should [illegible] in the denominator.

Appendix III

FIRST LEG ATTENUATION FACTOR, BASED ON DOSE 3 FEET ABOVE INFINITE PLANE

At the distance L_1 down the first leg, the dose from the rectangular entranceway with the isotropic source distributed equally across it is practically the same as that from a circular disc of the same area, provided the variation between the values of W_1 and H is not too extreme. A disc of this area would have a radius equal to $\sqrt{W_1 H/\pi}$. From Section 4.12 of Reference 6, Equation 4.12.1a indicates that the dose at distance L is approximately:

$$D_1 = J' \frac{W_1 H}{2\pi L_1^2} \qquad \text{(III-1)}$$

where J' is a factor, depending on source strength and energy, which provides numerical answers in proper units of dose or dose rate.

A rather accurate formula for dose readings in air, 3 feet above a smooth, infinite plane, homogeneously contaminated by a distributed radiation source, is given (Ref. 9) as follows:

$$D_p = J' \left[-E_i(-3\mu_{air}) + A_1 e^{-3B_1\mu_{air}} + A_2 e^{-3B_2\mu_{air}} \right] \qquad \text{(III-2)}$$

where μ_{air} is the total absorption coefficient in reciprocal feet for the radiation in air; A_1, A_2, B_1, and B_2 are empirical coefficients to account for the scattering contribution (Ref. 10); and E_i is the exponential integral (Ref. 11).

Using an energy value of 1 Mev for the photons, we can readily calculate that

$$D_p = 5.36\ J' \qquad \text{(III-3)}$$

The factor 5.36 is dependent on photon energy, but to a rather slowly varying extent. It will therefore be sufficiently accurate to consider it as representative for any practical situation of this sort.

Then the first leg attenuation factor, based on the dose at a reference point 3 feet above a smooth, infinite, contaminated plane, is:

$$F' = \frac{D_1}{D_p} \qquad \text{(III-4a)}$$

$$\cong \frac{W_1 \ H}{34 \ {L_1}^2} \qquad \text{(III-4b)}$$

UNCLASSIFIED

UNCLASSIFIED